

IMAGE RECONSTRUCTION WITH BACK FILTERED PROJECTION ALGORITHMS, USED IN CULTURAL HERITAGE INVESTIGATIONS

C. ARMEANU

National Institute of Research and Development in Optoelectronics INOE 2000, Romania
E-mail: Catalin.Armeanu@inoe.ro

Received July 30, 2015

Abstract. The software's that are currently used in 3D image reconstruction are usually presented as a so called "black box", which contains usually more algorithms. These algorithms are used in mathematics software like MatLab®, Mathematica®, Maple® and other. MatLab®, among others contain a very advanced module for image analysis and in the present work it will be presented a reconstruction of a test image using a back filtered projection (BFP) method, based on the Radon transform. Also we will analyze the image recomposed with 18, 36 and 90 projections.

Key words: image reconstruction, Radon, cultural heritage.

1. INTRODUCTION

Since the discovery of X rays, the field of application has extended from medical examinations to security control, but also in the field of cultural heritage investigations.

In art, radiology is used in the study of conservation, for identifying previous restoration attempts or even to study the working technique used by the artist.

There are cases when only a radiogram is good enough for investigating certain objects, but, there are many situations when it is required to have a 3D reconstruction of the object's image.

In order to obtain a 3D image of the object, we need a number of projections around the object. Using a back filtered projection algorithm, applied over each projection, the 3D image will be reconstructed. The present paper will discuss, using MatLab®'s Image Processing Toolbox and a test image, the optimal number of projections needed for a clear 3D image.

Besides other data obtained in 2D and reconstructed in 3D images, X-ray scanning is a widely used technique in cultural heritage investigations because of the importance of the information it gives us. Practically by using the reconstruction techniques we can reproduce from the 2D images, the 3D image of

the studied object, being able to observe by a noncontact manner, all the inside of an object. [3]

In art, it can be used X-ray scanning to reveal hidden defects, precious conservation hints, and even previous paintings under the visible layer. It can also identify certain use of some pigments and directing to a further spectroscopic analysis [7]. In historical artifacts imaging, it can give important information about the technology used by artists, previous conservations, degraded areas and causes of the degradation.

X-ray scanning has a very important role in cultural heritage investigations, among many other techniques like LIBS (Laser Induced Breakdown Spectroscopy) [8] and LIF (Laser Induced Fluorescence) or multi-spectral imaging. Altogether the techniques of investigation can produce a wide set of essential information for the cultural heritage studies [9].

Radiology can be seen as a complementary investigation in any study that is meant to observe also the insights of the object studied along with other imagistic techniques or spectroscopic analysis [10].

X-ray methods do not generate three dimensional images of an object directly. It provides 1 or 2 dimensional projections of the studied object. Hence, images have to be reconstructed from a set of projections. Real-world application needs image reconstruction from X-ray absorption projections obtained by measuring the radiation attenuation by crossing through a physical object at different angles [2]. Digitalized projections are collected by X-ray devices connected to computers and after that acquisition a virtual image of the object is reconstructed using different mathematical reconstruction methods. Energy of any given beam (not only X-ray beam) is absorbed depending on what it cross on its way between the source to the detector. This projection can be represented as an integral. Projection does not carry enough information to reconstruct an image, but it is a good starting point to build using mathematical methods to complete an image that approximate good enough the studied object [4].

2. RADON TRANSFORM

The Radon transform is named after Johann Radon [1], who showed in 1917 in a pure theoretical way with no association to applications, how to describe a function using its integral projections. The application from the function onto the projections is the so called Radon transform. The inverse Radon transform is used to the reconstruction process of the function from the integral projections obtained by measuring the attenuation of X-ray radiation that passes through a physical object at different angles.

We will use the following notations and definitions: x and y will denote the spatial coordinates; $I(x)$ is the D -dimensional image containing the

N -dimensional shapes; p denotes the vector containing the curve parameters; $c(p)$ is the member of a class of shapes described by the parameter vector p ; $c(s; p)$ are the coordinates of a point belonging to the shape $c(p)$; $C(x; p)$ will be the set of constraint functions that define a shape.

The number of constraint functions depends on the dimension of the shape. It is needed $D - N$ constraints to describe an N -dimensional shape. For a point on the shape, the constraint functions will be zero. The template $C(x, p)$ is also called the kernel that defines the shape defined by p as an image with spatial coordinates x . Image I can be modeled as a sum of some of these templates.

Observe that the parameters subset contains also the location of the shape (like the center of a sphere), hence we will write $p = \{q, x_0\}$, where x_0 is the location parameter of the shape and q the rest of the parameters.

The classical formulation of the Radon transform is:

$$R\{I\}(d, \phi) = \int_{\mathbb{R}} I(d \cos \phi - s \sin \phi, d \sin \phi + s \cos \phi) ds. \quad (1)$$

Even that initially it was an important but pure theoretical result, the Radon transform is known for its role in reconstruction of radiology scanning. Radon transform is used in the process of acquiring projections of an original object using X-rays. Given a set of projection data, we can use the inverse Radon transform to reconstruct the original object. Also, the Radon transform can be used for shape and pattern recognition. We can reformulate the Radon transform for a simpler use:

$$\begin{aligned} R\{I\}(d, \phi) &= \int_{(x,y)} I(x, y) dx dy \\ &= \int_{\mathbb{R}^2} I(x, y) \delta(x \cos \phi + y \sin \phi - d) dx dy. \end{aligned} \quad (2)$$

We can use another equivalent formulation, useful for some applications:

$$\begin{aligned} R_{c(p)}\{I\}(P) &= \int_{x \text{ on } c(p)} I(x) dx = \int_{\mathbb{R}^N} I(c(s; p)) \left\| \frac{\partial c}{\partial s} \right\| ds = \\ &= \int_{\mathbb{R}^D} I(x) \delta(c(x; p)) dx. \end{aligned} \quad (3)$$

They are other formulations, that are particularly practical in image analysis, that expresses the Radon transform in terms of a volume integral [5].

Imagine now that in the image there is a shape with parameter set a . If $p \neq a$, the Radon transform will evaluate the number of intersections between the shapes $c(p)$ and $c(a)$. When $p = a$, the Radon transform offer a peak in the parameter space. This result is proportional to the N -dimensional hyper-volume of the shape. The Radon transform can be interpreted as follows: it provides a function from

image space to the parameter space generated by the parameters p . Function $P(p)$ created in this parameter space contains the peaks of those p for which the shape $c(p)$ is found in the image. Therefore, the shape detection problem is reduced using Radon transforms to the much simpler problem of peak detection.

Equation (4) form of the Radon transform shows an important reason for using distributions (generalized functions). In this formulation, it can be recognized the form of a linear integral operator, also known as a Fredholm operator, L_C with kernel C :

$$(L_C I)(p) = \int_{\mathbb{R}^D} C(p, x) I(x) dx. \quad (4)$$

Hence, if we allow for the kernel C to be a distribution, the Radon transform can be used as any other linear transformation. Using distributions, the identity operator can be described in integral form. In order to develop a continuous equivalent to matrix algebra, Dirac introduced these in his work on quantum mechanics.

For the Radon transform, the kernel C takes the form:

$$C(p, x) = \delta(c(x; p)). \quad (5)$$

In shape detection, the operator L_C is used to compute the inner product between a template C the image and the image for a given parameter set p . Usually, the parameters p consists of the position of the shape x_0 and the actual shape parameters q . In this situation, the kernel has a special structure:

$$C(\{q, x_0\}x) = C(\{q, x_0 + d\}, x + d), \quad (6)$$

for any d .

The operator L_C now reduces to a set of convolutions:

$$(L_C I)(q, x_0) = (K_C(q) * xI)(x_0), \quad (7)$$

with $K_C(q, x) = C(\{q, x\}, 0)$.

This brings a large speed-up for the computing process because each convolution becomes a multiplication in the Fourier domain, using the convolution property of the Fourier transform.

In MatLab® the Image Processing Toolbox, has an already built in function for the Radon inverse transform, *iradon*. It is important to know that MatLab® reads an image as a matrix and therefore all the operations that can be applied to matrices can also be applied to images [6].

The *iradon* function inverts the Radon transform and hence can be used to reconstruct images.

Given any image I and a set of fixed projection angles θ , the Radon function can be used to compute the Radon transform

$$R = \text{radon}(I, \theta);$$

Then, the function *iradon* can be used to reconstruct from his projection data the image I

$$IR = \text{iradon}(R, \theta);$$

In the below presented example, we will calculate the projections from the original image I.

However, in applications, we don't have the original image, but we have the projections of the image and the purpose is to construct an image from these projections. This is the situation in tomography applications where the inverse Radon transform is commonly used. Or in X-ray absorption tomography, when the projections are obtained by measuring the absorption of radiation that cross through a physical object at different angles. We can reconstruct the original image from the cross sections through the object, where intensity values obtained represent the density of the object. Projections are obtained using special x-ray hardware, then an image of the object is reconstructed by *iradon*. This allows a noninvasive imaging of the inside of an opaque object.

Function *iradon* reconstructs images from parallel-beam projections. Parallel-beam geometry uses projection obtained by compounding a collection of line integrals throughout an image at a specific, constant angle.

Figure 1 illustrates how parallel-beam geometry is used in X-ray absorption tomography. There are an equal number n of emitters and n corresponding sensors. Each sensor measures the attenuation of the radiation emitted from its corresponding emitter. The attenuation of the radiation gives information and measure the density of the object. This match to the line integrals that are calculated in the Radon transform presented before.

Figure 1 shows the parallel-beam geometry which is in fact the geometry that was described in Radon Transform. The function $f(x,y)$ describe the luminosity of the image and $R_{\theta}(x')$ is the theta angle projection of the object.

Function *iradon* uses a filtered backprojection algorithm to work out the inverse Radon transform. The filtered backprojection algorithm reconstruct an approximation of the original image I using the projections represented as the columns of R . A better result, as we will see, can be obtained using more projections at smaller angles. As the number of projections increases, and hence smaller theta, the reconstructed image IR approximates more accurately the original image I . The vector theta can contain increasing angular values with a constant growing angle $D\theta$. The scalar $D\theta$ can be used to the function *iradon* instead of the vector of theta values. For example:

$$IR = \text{iradon}(R, D\theta).$$

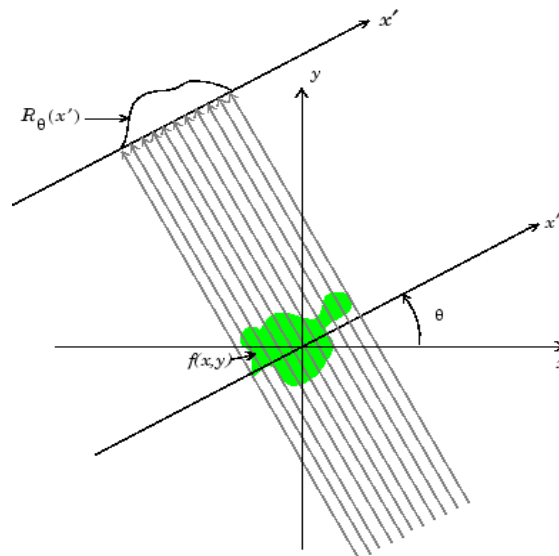


Fig. 1 – Parallel-beam projections throughout an object.

Usually, the filtered backprojection algorithm first filters the projections of R and secondly reconstructs the image using the filtered projections. However, there is always some noise in the projections. Sometimes, this noise must be attenuated. To attenuate for example high frequency noise, we can apply a window to the filter. Windowed filters are available in `iradon`. Next example applies a Hamming window to `iradon`

$$IR = \text{iradon}(R, \text{theta}, \text{'Hamming'}).$$

Function `iradon` enables us to use an above normalized frequency D . The value D is a scalar in $[0, 1]$. Above D the filter has zero response. Using this option, the frequency axis is rescaled such that the filter is compressed into the frequency range $[0, D]$. This is very useful when the projections carry little high-frequency information but there is present a high-frequency noise. In this situation, the noise can be even completely deleted without endanger the quality of reconstruction. The following use of `iradon` shows how to set 0.85 as normalized frequency

$$IR = \text{iradon}(R, \text{theta}, 0.85).$$

Now we shall reconstruct an Image from Parallel Projection Data.

The example below illustrates how to reconstruct and compare an image from parallel projection data. We will use as test image the Shepp-Logan phantom, which can be generated using the phantom function.

First we can create a Shepp-Logan head phantom image by:

```
P = phantom (256);  
imshow (P)
```



Fig. 2 – Shepp-Logan phantom image.

Now we compute the Radon transform of the Shepp-Logan phantom for three different sets of values for theta. First application R01 has 18 projections with $D\theta = 10^\circ$, second application R02 has 36 projections with $D\theta = 5^\circ$, and third application R03 has 90 projections and $D\theta = 2^\circ$

1. $\theta_{01} = 0:10:170$; $[R_{01}, xp] = \text{radon}(P, \theta_{01})$;
2. $\theta_{02} = 0:5:175$; $[R_{02}, xp] = \text{radon}(P, \theta_{02})$;
3. $\theta_{03} = 0:2:178$; $[R_{03}, xp] = \text{radon}(P, \theta_{03})$;

Next step is to reconstruct and display the results for the phantom image from the projection data created in the previous step

4. $I_1 = \text{iradon}(R_{01}, 10)$;
5. $I_2 = \text{iradon}(R_{02}, 5)$;
6. $I_3 = \text{iradon}(R_{03}, 2)$;
7. $\text{imshow}(I_1)$
8. $\text{figure, imshow}(I_2)$
9. $\text{figure, imshow}(I_3)$

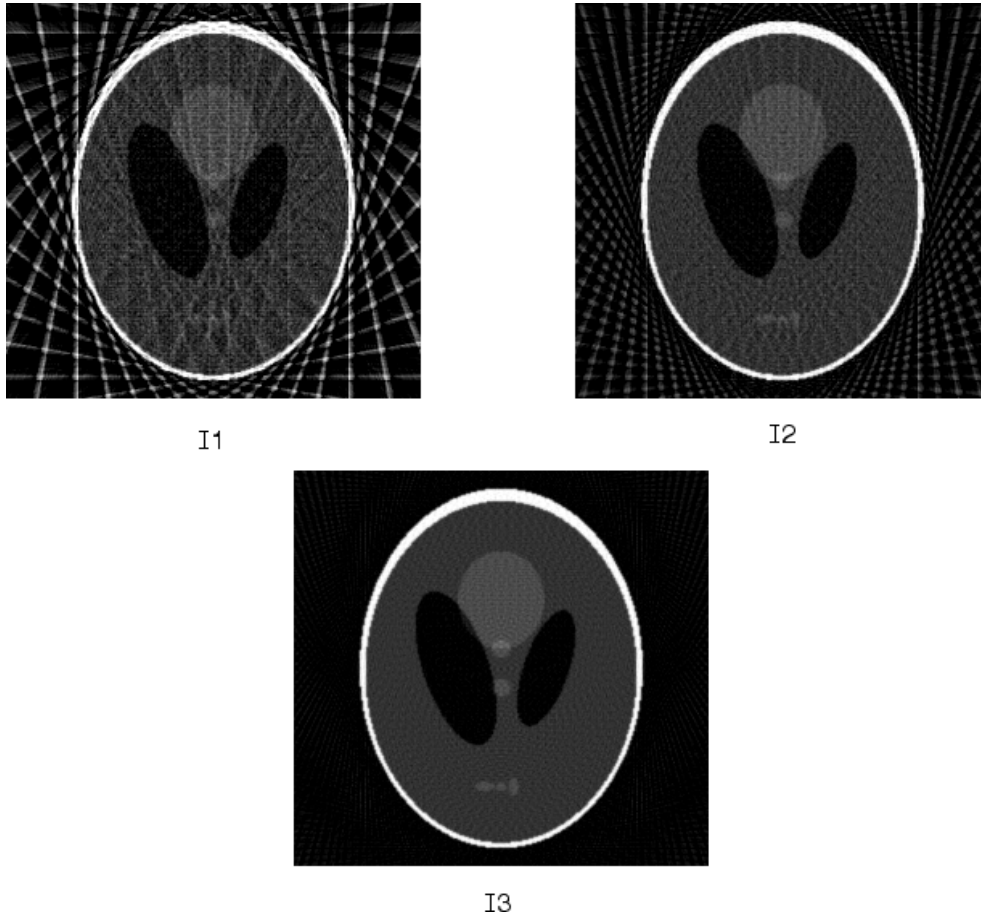


Fig. 3 – I1 is the image of R01 reconstructed from 18 projections for $D\theta = 10^\circ$,
I2 – is the image of R02 reconstructed from 36 projections and $D\theta = 5^\circ$ and
I3 is the image of R03 reconstructed from 90 projections with $D\theta = 2^\circ$.

Discussion. Comparing the resulted images with the original Shepp-Logan phantom it is easy to observe that image I1, that was reconstructed from 18 projections and big $D\theta = 10^\circ$, as expected, is the least precise reconstruction. Image I2, reconstructed from 36 projections and $D\theta = 5^\circ$, is much better, but still not clear enough to recognize clearly the small ellipses in the bottom of the image. The image I3, reconstructed using 90 projections and $D\theta = 2^\circ$, most closely approximates the original image. The conclusion is that for a small number of projections (as in image I1 and image I2), the reconstruction is not accurate and can include some artifacts and noise from the back projection. The best quality is obtained in I3, where the number of projections is the highest. On the other hand,

we can observe, that at a much higher number of projections the center of the image will be very dense, because all the projections are intersecting at the center.

Acknowledgements. The presented activities are part of the national project CERES, funded by ANCS, CNDI – UEFISCDI, Partnerships in priority domains, project number: PN-II-PT-PCCA-2013-4-0495.

REFERENCES

1. J. Radon, *Über die Bestimmung von Funktionen durch ihre Integralwerte längs gewisser Mannigfaltigkeiten*, Berichte über die Verhandlungen der Königlich-Sächsischen Akademie der Wissenschaften zu Leipzig, Mathematisch-Physische Klasse, Teubner, Leipzig, 1917.
2. A. C. Kak, M. Slaney, *Principles of Computerized Tomographic Imaging*, New York, IEEE Press, 1988.
3. R. N. Bracewell, *Two-Dimensional Imaging*, Englewood Cliffs, Prentice Hall, 1995.
4. J.S. Lim, *Two-Dimensional Signal and Image Processing*, Englewood Cliffs, Prentice Hall, 1990.
5. S. R. Deans, *The Radon Transform and Some of Its Applications*, New York, John Wiley & Sons, 1983.
6. A. McAndrew, *An Introduction to Digital Image Processing with Matlab; Notes for SCM2511 Image Processing 1, Semester 1*, School of Computer Science and Mathematics, Victoria University of Technology, 2004.
7. M. Simileanu, R. Radvan, D. Pandrea, *Evaluation of the conservation status of the fountain ensemble from Braila's Trajan square, using laser induced breakdown spectroscopy*, Politehnica University of Bucharest, Scientific Bulletin – Series A – Applied Mathematics and Physics, 2014.
8. M. Simileanu, W. Maracineanu, J. Striber *et al.*, *Advanced research technology for art and archaeology – ART4ART mobile laboratory*, Journal of Optoelectronics and Advanced Materials, 2008.
9. M. Simileanu, R. Radvan, N. Puscas, *Underwater LIBS investigations setup for metals' identification*, Politehnica University of Bucharest, Scientific Bulletin – Series A – Applied Mathematics and Physics, 2010.
10. M. Simileanu, W. Maracineanu, C. Deciu *et al.*, *A complex portable optoelectronic setup for on site interventions – Case studies – art. no. 63450U*, Seventh International Conference on Vibration Measurements by Laser Techniques, 2006.

